ISSN 2181-8622

Manufacturing technology problems

Scientific and Technical Journal Namangan Institute of Engineering and Technology

INDEX COPERNICUS INTERNATIONAL

Google Scholar

Crossref doi

SLIB.UZ
Scientific library of Uzbekistan

Volume 11
Issue 1
2026

NamMTI ILMIY-TEXNIKA JURNALI TAHRIR HAY'ATI A'ZOLARI

Bosh muharrir: f-m.f.d., prof. O.O. Mamatkarimov

Bosh muharrir o'rinbosari: k.f.d., prof. O.K. Ergashev

TEXNIKA FANLARI (PAXTA, TO'QIMACHILIK VA YENGIL SANOAT)

1. Prof. Dr. Metin ÇOLAK – *Ege Universiteti, Turkiya*
2. Prof. Dr. Suneel KATERIYA – *Javoharlal Nehru Universiteti, Hindiston*
3. Prof. Dr. Muradov RUSTAM – *Namangan To'qimachilik Sanoat Instituti*
4. Prof. Dr. Obidov AVAZBEK – *Namangan Muhandislik-Texnologiya Instituti*
5. Prof. Dr. Maxkamov ANVAR – *Namangan Muhandislik-Texnologiya Instituti*
6. Prof. Dr. Azizov SHUXRAT – *Namangan Muhandislik-Texnologiya Instituti*
7. Dr. Qorabayev SHERZOD – *Namangan Muhandislik-Texnologiya Instituti*

TEXNIKA FANLARI (QISHLOQ XO'JALIGI VA OZIQ-OVQAT TEXNOLOGIYALARI)

1. Prof. Dr. Sakina BINTU ABDULLAH – *Malaya Universiteti, Malayziya*
2. Prof. Dr. Abdalova GULISTAN – *Taraz davlat universiteti, Qozog'iston*
3. Prof. Dr. Xudayberdiyev ABSALOM – *Namangan muhandislik-texnologiya instituti*
4. Prof. Dr. Merganov AVAZXON – *Namangan muhandislik-texnologiya instituti*
5. Prof. Dr. Sherquziyev DONIYOR – *Namangan muhandislik-texnologiya instituti*
6. Prof. Dr. Qanoatov XAYRULLO – *Namangan muhandislik-texnologiya instituti*
7. Prof. Dr. Mamatov SHERZOD – *Toshkent shahridagi Vebster Universiteti*

TEXNIKA FANLARI (MEXANIKA VA MASHINASOZLIK)

1. Dr. Jaclyn SHARP – *Pittsburg Universiteti, AQSH*
2. Prof. Dr. Aleksey KAZINSKY – *Saratov davlat texnologiya universiteti, Rossiya*
3. Akad. Prof. Zaynobiddinov SIROJIDDIN – *Andijon Davlat Universiteti*
4. Prof. Dr. Usmanov PAZLITDIN – *Namangan muhandislik-texnologiya instituti*
5. Prof. Dr. Matkarimov PAXRIDDIN – *Namangan muhandislik-texnologiya instituti*
6. Prof. Dr. Sharibayev NOSIRJON – *Namangan muhandislik-texnologiya instituti*
7. Prof. Dr. Erkaboyev ULUG'BEK – *Namangan muhandislik-texnologiya instituti*

KIMYO FANLARI (KIMYO VA KIMYOVIY TEXNOLOGIYALAR)

1. Prof. Dr. Abel SANTOS – *Porto Universiteti, Portugaliya*
2. Prof. Dr. Junli YANG – *Lanzhou kimyoviy fizika instituti, Xitoy*
3. Akad. Prof. Namazov ShAFOAT – *O'zR FA Umumiy va Noorganik Kimyo instituti*
4. Prof. Dr. Botirov ERKIN – *O'zR FA O'simlik Moddalar Kimyosi Instituti*
5. Prof. Dr. Akbarov HAMDAM – *O'zbekiston Milliy Universiteti*
6. Prof. Dr. Nurmanov SUVANKUL – *O'zbekiston Milliy Universiteti*
7. Prof. Dr. Salihanova DILNOZA – *O'zR FA Umumiy va Noorganik Kimyo instituti*
8. Prof. Dr. Kattayev NURIDDIN – *O'zbekiston Milliy Universiteti*
9. Prof. Dr. Sultonov PO'LATJON – *Geologiya fanlari universiteti*

TA'LIMDA ILG'OR PEDAGOGIK TEXNOLOGIYALAR

1. Prof. Dr. Paul TIKALSKY – *Oklahoma Davlat Universiti, AQSH*
2. Dr. David Leffler – *Liberty Universiteti, AQSH*
3. Prof. Dr. Wen-Jian ZHANG – *Zhejiang Universiteti, China*
4. Prof. Ergashev ShARIBBOY – *Namangan Muhandislik-Qurilish Instituti*
5. Prof. Dr. Musayev JAHONGIR – *OFIV*
6. Prof. Dr. Eshbayeva ULBOSIN – *Namangan Muhandislik-Texnologiya Instituti*
7. Prof. Dr. Xoshimova DILDORA – *Namangan Muhandislik-Texnologiya Instituti*

IQTISODIYOT FANLARI

1. Dr. Biral MERCAN – *Necmettin Erbakan Universiteti, Turkiya*
2. Dr. Orsolya KATONA – *Miskolc Universiteti, Vengriya*
3. Prof. Dr. Soliyev AHMADJON – *Namangan Muhandislik-Texnologiya Instituti*
4. Prof. Dr. Saidboyev ShERMIRZA – *Namangan Muhandislik-Texnologiya Instituti*
5. Prof. Matkarimov KAMOLIDDIN – *Namangan Muhandislik-Texnologiya Instituti*
6. Dr. Bustonov MANSUR – *Namangan Muhandislik-Texnologiya Instituti*
7. Dr. Rashidov RAKHMATILLA – *Namangan Muhandislik-Texnologiya Instituti*

Muharrirlar guruhi
O. Kazakov, B. Xolmirzayev, A. Mirzaev, Sh. Mahsudov,
A. Tursunov, O. R. Qodirov (mas'ul muharrir)

ASSESSMENT OF THE CHEMICAL AND MINERALOGICAL PROPERTIES OF ROCKS FROM THE MOUNTAINOUS AREAS OF CHORTOQ DISTRICT, NAMANGAN REGION, BASED ON XRF AND FTIR METHODS

SULTANOV DAVRONBEK
PhD student, Namangan State Technical University, Namangan, Uzbekistan
Phone.: (0599) 324-0913, E-mail.: sultanovdavronbek653@gmail.com

MAMAHONOV AZAM
Professor, Namangan State Technical University, Namangan, Uzbekistan
Phone.: (0598) 772-7160, E-mail.: azamat0783@mail.com
**Corresponding author*

Abstract: This article investigates the chemical and mineralogical composition of rocks from the mountainous areas of Chortoq District, Namangan Region, using modern instrumental analytical methods, namely energy-dispersive X-ray fluorescence (XRF) and Fourier-transform infrared spectroscopy (FTIR). The elemental composition was evaluated in terms of the mass fractions of the major oxide-forming components, and the relative amount of the carbonate phase was calculated from the calcium content using a stoichiometric approach. Spectral identification of mineral phases was carried out based on FTIR spectra. In order to establish the relationship between chemical and mineralogical indicators and mechanical strength parameters, integrated indicators such as the silicate index (SI), carbonate intensity index (CI), and mineral strength index (MI) were proposed. The obtained results confirmed that an increase in the carbonate phase content has a positive effect on the structural compactness and mechanical strength of the rocks.

Keywords: rocks, XRF analysis, FTIR spectroscopy, chemical composition, mineral phase, carbonate content, silicate index, mechanical strength.

Introduction. A comprehensive investigation of the chemical and mineralogical composition of natural rocks is of great importance for the scientific interpretation of their physico-mechanical properties, the assessment of their potential for industrial and construction applications, and the evaluation of their long-term service stability. In particular, the relative proportions of carbonate and silicate phases, the distribution of iron-bearing and aluminosilicate components, as well as the presence of secondary mineral phases, directly influence the density, porosity, water–rock interaction, and strength properties of rocks.

The mountainous areas of Chortoq District are characterized by a geologically complex structure, and the rocks occurring in this region exhibit considerable compositional and structural variability. Determining the chemical composition of such rocks by instrumental methods, identifying their mineralogical phases by spectroscopic techniques, and correlating these indicators with mechanical strength results are essential for the scientific evaluation of regional raw material resources [1–2].

Among modern analytical techniques, energy-dispersive X-ray fluorescence (XRF) enables the relatively rapid, reliable, and accurate determination of the elemental composition of rocks. In particular, this method allows the evaluation of the major elements such as Ca, Si, Fe, Al, K, and Ti, making it possible to infer whether the rock has a predominantly carbonate or silicate nature. Fourier-transform infrared spectroscopy

(FTIR), in turn, is an effective technique for identifying mineral phases on the basis of functional group vibrations and provides spectral information on carbonate groups, hydroxyl zones, and silicate bonds [3].

The aim of the present study is to determine the chemical and mineralogical properties of rocks collected from the mountainous areas of Chortoq District, Namangan Region, using XRF and FTIR methods, to assess the ratio of carbonate and silicate phases, and to scientifically analyze their relationship with the levels of mechanical resistance. The objectives of the study were as follows:

1. To determine the elemental composition of rock samples using the XRF method;
2. To perform a stoichiometric estimation of the approximate mass fraction of the carbonate phase based on calcium content;
3. To identify the principal mineral-functional groups using FTIR spectra;
4. To calculate the silicate index, carbonate intensity index, and mineral strength index;
5. To analyze the relationship between chemical and spectral indicators and mechanical resistance.

The scientific novelty of this article lies in the fact that the chemical and mineralogical data of rocks from Chortoq District were evaluated in an integrated manner together with their mechanical strength levels, and the relationship between the increase in the carbonate component and the structural compactness and resistance of the rocks was demonstrated.

Research Objects and Methods. Three rock samples collected from the mountainous areas of Chortoq District were selected for the present study. Based on the results of previous physico-mechanical tests, the samples were conventionally classified into low, medium, and high mechanical resistance categories. Such grouping made it possible to comparatively evaluate the relationship between the chemical and mineralogical characteristics and the mechanical properties of the rocks.

A)

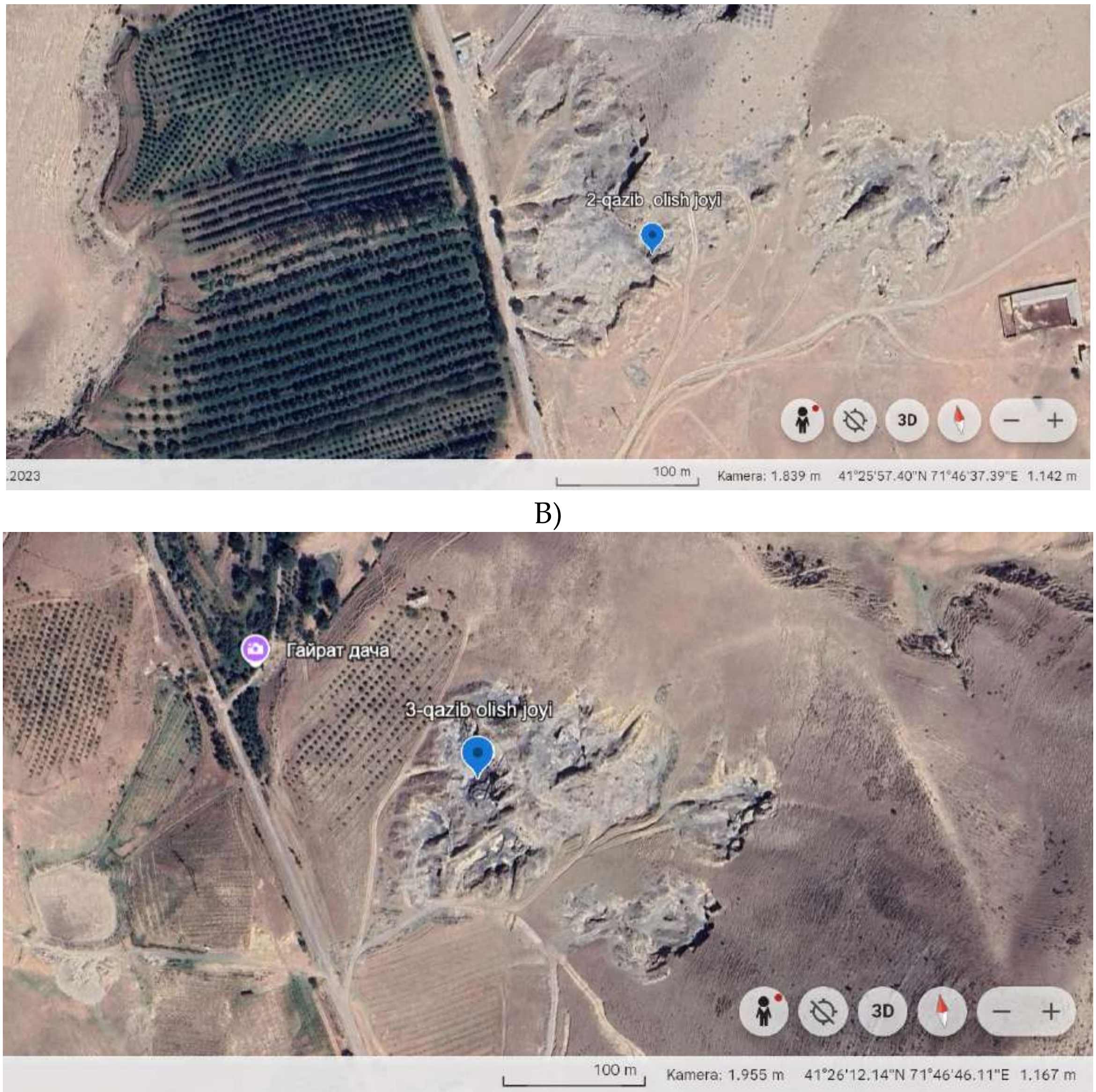

B)

C)

Figure 1. Sampling locations of the rock specimens

For the purposes of the present study, the samples were designated as follows: A – Sample 1, B – Sample 2, and C – Sample 3. The selection of the specimens was based on their macroscopic integrity, freedom from external contamination, relative homogeneity, and suitability for laboratory analysis. For XRF and FTIR analyses, the samples were crushed, dried, and prepared in accordance with analytical requirements.

XRF Analysis Method. The elemental composition of the rock samples was determined using the energy-dispersive X-ray fluorescence (XRF) method. The physical principle of this method is based on the excitation of the inner electron shells of atoms when the sample is irradiated with primary X-rays. As the atoms return to a stable state, secondary X-ray fluorescence characteristic of each element is emitted. By recording the energy and intensity of this radiation, both the qualitative and quantitative elemental composition can be determined from the resulting spectra [4].

A major advantage of the XRF method in rock studies is that it enables the rapid, relatively non-destructive, and highly accurate determination of major as well as certain trace elements in a sample. In particular, this method is highly effective for identifying the principal components of carbonate and silicate rocks, such as Ca, Si, Fe, Al, K, and Ti. Therefore, in geology, petrography, geochemistry, and construction materials science, XRF analysis is widely used as one of the key instrumental techniques for the preliminary and comparative evaluation of rock composition.

The analytical results were recorded as mass fractions of elements (wt.%). The main evaluated components included Ca, Si, Fe, Al, K, and Ti. In addition, the presence of elements such as Cl, S, Sr, and Mn was also detected. These supplementary elements provide additional geochemical information regarding the genesis of the rocks, secondary mineral transformations, alteration processes, and the composition of specific mineral phases. For example, Sr may be associated with carbonate environments, whereas Cl and S may be interpreted as possible indicators of saline or sulfate-related secondary processes.

Stoichiometric Estimation of the Carbonate Phase. The calcium content was taken as the principal indicator of the carbonate phase. Assuming that calcium in the rock occurs predominantly in the form of calcium carbonate, the approximate amount of the carbonate phase can be estimated using a stoichiometric relationship:

$$CaCO_3 \approx Ca \cdot \frac{M(CaCO_3)}{M(Ca)} \tag{1}$$

where $M(CaCO_3) = 100.9$g/mol and $M(Ca) = 40.8$g/mol.

Thus:

$$\frac{M(CaCO_3)}{M(Ca)} = \frac{100.9}{40.8} \approx 2.497$$

Accordingly, the approximate mass fraction of the carbonate phase can be expressed as follows:

$$CaCO_3(\%) \approx 2.497 \cdot Ca(\%)$$

This approach does not represent the absolute mineralogical composition, but rather provides a rapid estimate of the relative proportion of the carbonate component. If calcium is also incorporated into other mineral phases, such as plagioclases, pyroxenes, or sulfate compounds, the actual carbonate content may differ from the calculated value [4].

Silicate Coefficient. In order to assess the mixed silicate–carbonate nature of the rock, a silicate index was introduced:

$$SI = \frac{Si+Al}{Ca} \tag{2}$$

where Si, Al, and Ca are the corresponding elemental mass fractions (wt.%).

This coefficient expresses the relative abundance of aluminosilicate components with respect to calcium in the rock composition. A higher SI value indicates a stronger predominance of silicate and aluminosilicate phases. Conversely, a decrease in SI suggests a relatively greater contribution of the carbonate phase. This parameter is a convenient dimensionless index for the comparative evaluation of the mineralization character of rocks.

FTIR Spectroscopic Analysis. FTIR was used to identify mineral phases and functional groups. The spectra were recorded in the range of 4000–500 cm⁻¹. This spectral range covers the principal absorption bands characteristic of carbonate groups, hydroxyl-bearing compounds, and silicate bonds.

The main vibrations characteristic of the carbonate group are as follows:

- ν_3(1400–1500 cm⁻¹) — asymmetric stretching vibration of the CO_3^{2-}group;
- ν_2(~875 cm⁻¹) — out-of-plane deformation vibration;
- ν_4(~710 cm⁻¹) — in-plane deformation vibration.

The relative spectral intensity of the carbonate phase was evaluated using the following parameter:

$$CI = \frac{A(\nu_3)}{A_{total}} \tag{3}$$

where:

- CI is the carbonate intensity index;
- $A(\nu_3)$is the integrated area of the $\nu_3$peak;
- $A_{total}$is the total integrated area of the spectrum.

In addition, the broad absorption band in the range of 3400–3800 cm⁻¹ was recorded as a qualitative indicator of the presence of hydroxyl groups or adsorbed water. Certain peaks in the range of 600–1100 cm⁻¹, characteristic of Si–O bonds, were interpreted as silicate indicators.

Mineral–Mechanical Integrated Parameter. In order to more comprehensively represent the relationship between chemical composition and mechanical resistance, a mineral strength index was proposed:

$$MI = \frac{CaCO_3}{Si+Fe} \tag{4}$$

where $CaCO_3$is the stoichiometrically estimated carbonate content (%) based on the XRF data, and Si and Fe are the main components representing the relatively hard yet heterogeneous structure of the rock (wt.%).

The physical significance of this index is that an increase in the carbonate component together with a relative decrease in silicate- and iron-bearing constituents may lead to greater compactness of the internal rock structure. Therefore, an increase in MI is expected to correspond to higher mechanical resistance [5].

Statistical Analysis. The relationship between elemental composition and mechanical parameters was evaluated using the Pearson correlation coefficient:

$$r = \frac{\sum[(x_i-\bar{x})(y_i-\bar{y})]}{\sqrt{\sum(x_i-\bar{x})^2\sum(y_i-\bar{y})^2}} \tag{5}$$

where $x$denotes a chemical or spectral parameter and $y$represents a mechanical strength parameter.

This statistical approach was used to determine the direction and relative strength of the relationship. Since the number of samples in this study was limited, the correlation results were used primarily to indicate trends and were interpreted with caution.

Table 1. XRF analysis results (wt.%)

No.	Mechanical grade	Ca (%)	Si (%)	Fe (%)	Al (%)	K (%)	Ti (%)	Cl (%)	S (%)	Sr (%)	Mn (%)
1	Low	38.731	27.233	16.724	5.183	6.428	1.630	2.104	1.113	0.238	0.163
2	Medium	52.796	26.002	11.048	4.252	2.858	1.062	0.328	0.191	0.460	0.290
3	High	59.132	23.523	10.087	2.454	1.690	1.561	0.359	0.052	0.522	0.334

The XRF results indicate significant differences in the chemical composition of the samples. The most notable trend is the progressive increase in calcium content from the sample with low mechanical grade to that with high mechanical grade. In Sample 1, Ca accounted for 38.731 wt.%, whereas in Sample 2 this value increased to 52.796 wt.%, and in Sample 3 it reached 59.132 wt.%. This suggests that the samples with higher mechanical resistance are enriched in the carbonate component.

Conversely, the contents of Si, Fe, and Al decreased with increasing mechanical grade. Specifically, Si decreased from 27.233 wt.% to 23.523 wt.%, Fe from 16.724 wt.% to 10.087 wt.%, and Al from 5.183 wt.% to 2.454 wt.%. This trend indicates that aluminosilicate and iron-bearing phases become relatively less abundant, while the carbonate component becomes more dominant [5].

The decrease in K content from 6.428 wt.% to 1.690 wt.% may likewise indicate a reduction in silicate phases, particularly feldspar or other K-bearing minerals. The Ti content varied within a relatively narrow range, suggesting the presence of accessory minerals. The higher contents of Cl and S in Sample 1 may be associated with secondary alteration, saline impurities, or surface weathering processes.

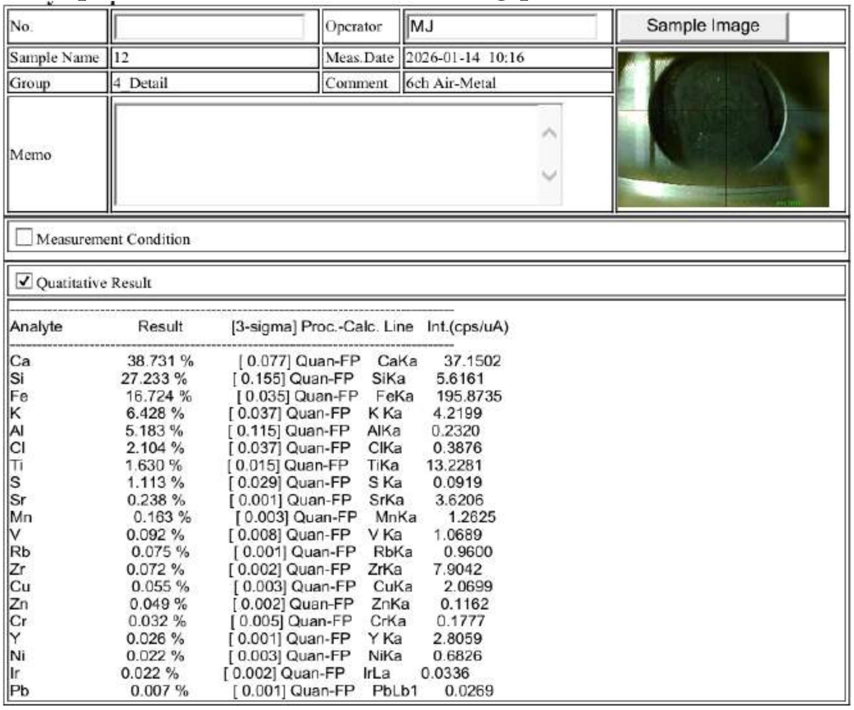

No.		Opcrator	MJ
Sample Name	12	Meas.Date	2026-01-14 10:16
Group	4_Detail	Comment	6ch Air-Metal
Memo			

☐ Measurement Condition

☑ Quatitative Result

```
--------------------------------------------------------------------------
Analyte        Result      [3-sigma] Proc.-Calc. Line  Int.(cps/uA)
--------------------------------------------------------------------------
Ca            38.731 %      [ 0.077] Quan-FP   CaKa    37.1502
Si            27.233 %     [ 0.155] Quan-FP   SiKa    5.6161
Fe            16.724 %      [ 0.035] Quan-FP   FeKa    195.8735
K              6.428 %     [ 0.037] Quan-FP   K Ka    4.2199
Al             5.183 %     [ 0.115] Quan-FP   AlKa    0.2320
Cl             2.104 %     [ 0.037] Quan-FP   ClKa    0.3876
Ti             1.630 %     [ 0.015] Quan-FP   TiKa   13.2281
S              1.113 %     [ 0.029] Quan-FP   S Ka    0.0919
Sr             0.238 %     [ 0.001] Quan-FP   SrKa    3.6206
Mn              0.163 %     [ 0.003] Quan-FP   MnKa     1.2625
V              0.092 %     [ 0.008] Quan-FP   V Ka    1.0689
Rb              0.075 %     [ 0.001] Quan-FP   RbKa     0.9600
Zr             0.072 %     [ 0.002] Quan-FP   ZrKa    7.9042
Cu              0.055 %     [ 0.003] Quan-FP   CuKa     2.0699
Zn             0.049 %     [ 0.002] Quan-FP   ZnKa    0.1162
Cr             0.032 %     [ 0.005] Quan-FP   CrKa    0.1777
Y              0.026 %     [ 0.001] Quan-FP   Y Ka    2.8059
Ni             0.022 %     [ 0.003] Quan-FP   NiKa    0.6826
Ir            0.022 %     [ 0.002] Quan-FP   IrLa   0.0336
Pb              0.007 %     [ 0.001] Quan-FP   PbLb1    0.0269
```

A)

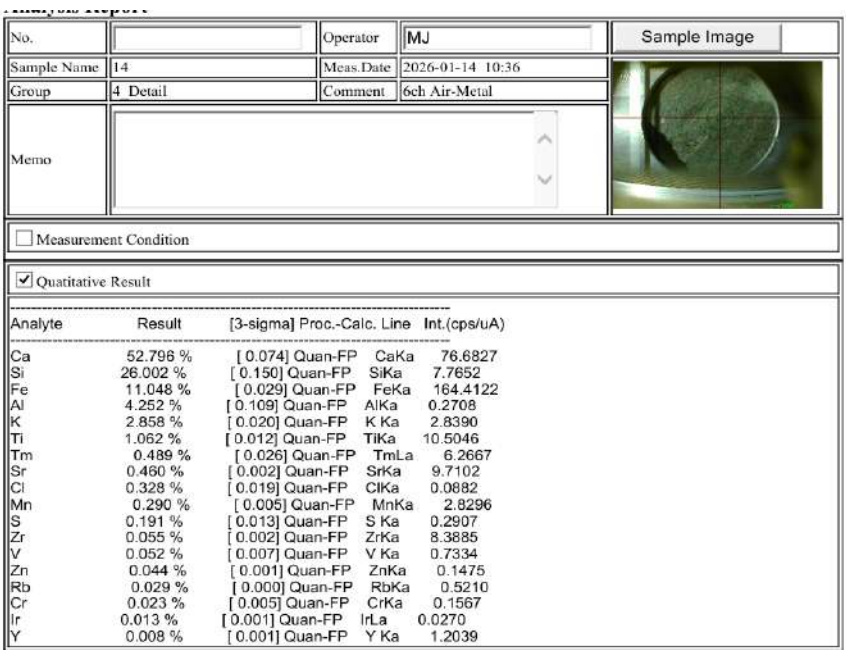

No. | Operator MJ | Sample Image
Sample Name 14 | Meas.Date 2026-01-14 10:36
Group 4_Detail | Comment 6ch Air-Metal
Memo

☐ Measurement Condition

☑ Quatitative Result

```
Analyte        Result      [3-sigma] Proc.-Calc. Line  Int.(cps/uA)
Ca            52.796 %     [0.074] Quan-FP   CaKa    76.6827
Si            26.002 %     [0.150] Quan-FP   SiKa    7.7652
Fe            11.048 %     [0.029] Quan-FP   FeKa    164.4122
Al             4.252 %     [0.109] Quan-FP   AlKa    0.2708
K              2.858 %     [0.020] Quan-FP   K Ka    2.8390
Ti             1.062 %     [0.012] Quan-FP   TiKa    10.5046
Tm             0.489 %     [0.026] Quan-FP   TmLa    6.2667
Sr             0.460 %     [0.002] Quan-FP   SrKa    9.7102
Cl             0.328 %     [0.019] Quan-FP   ClKa    0.0882
Mn             0.290 %     [0.005] Quan-FP   MnKa    2.8296
S              0.191 %     [0.013] Quan-FP   S Ka    0.2907
Zr             0.055 %     [0.002] Quan-FP   ZrKa    8.3885
V              0.052 %     [0.007] Quan-FP   V Ka    0.7334
Zn             0.044 %     [0.001] Quan-FP   ZnKa    0.1475
Rb             0.029 %     [0.000] Quan-FP   RbKa    0.5210
Cr             0.023 %     [0.005] Quan-FP   CrKa    0.1567
Ir             0.013 %     [0.001] Quan-FP   IrLa    0.0270
Y              0.008 %     [0.001] Quan-FP   Y Ka    1.2039
```

B)

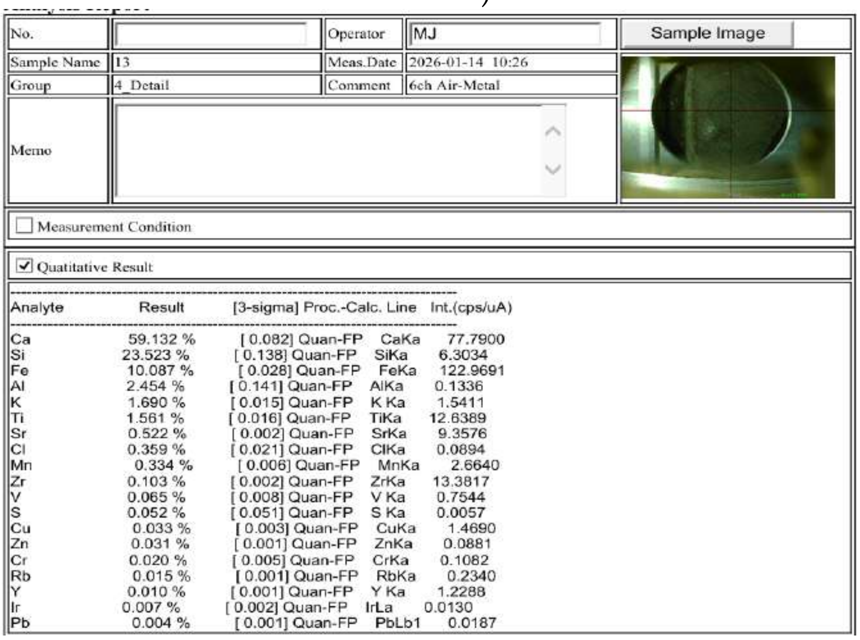

No. | Operator MJ | Sample Image
Sample Name 13 | Meas.Date 2026-01-14 10:26
Group 4_Detail | Comment 6ch Air-Metal
Memo

☐ Measurement Condition

☑ Quatitative Result

```
Analyte        Result      [3-sigma] Proc.-Calc. Line  Int.(cps/uA)
Ca            59.132 %     [0.082] Quan-FP   CaKa    77.7900
Si            23.523 %     [0.138] Quan-FP   SiKa    6.3034
Fe            10.087 %     [0.028] Quan-FP   FeKa    122.9691
Al             2.454 %     [0.141] Quan-FP   AlKa    0.1336
K              1.690 %     [0.015] Quan-FP   K Ka    1.5411
Ti             1.561 %     [0.016] Quan-FP   TiKa    12.6389
Sr             0.522 %     [0.002] Quan-FP   SrKa    9.3576
Cl             0.359 %     [0.021] Quan-FP   ClKa    0.0894
Mn             0.334 %     [0.006] Quan-FP   MnKa    2.6640
Zr             0.103 %     [0.002] Quan-FP   ZrKa    13.3817
V              0.065 %     [0.008] Quan-FP   V Ka    0.7544
S              0.052 %     [0.051] Quan-FP   S Ka    0.0057
Cu             0.033 %     [0.003] Quan-FP   CuKa    1.4690
Zn             0.031 %     [0.001] Quan-FP   ZnKa    0.0881
Cr             0.020 %     [0.005] Quan-FP   CrKa    0.1082
Rb             0.015 %     [0.001] Quan-FP   RbKa    0.2340
Y              0.010 %     [0.001] Quan-FP   Y Ka    1.2288
Ir             0.007 %     [0.002] Quan-FP   IrLa    0.0130
Pb             0.004 %     [0.001] Quan-FP   PbLb1   0.0187
```

C)

Figure 1. XRF chemical element analysis for locations A, B, and C.

Stoichiometric Estimation of the Carbonate Phase. Based on the Ca content, the approximate carbonate phase content was calculated as follows:

- Sample 1:

$$CaCO_3 \approx 2.497 \times 38.731 = 96.73\%$$

- Sample 2:

$$CaCO_3 \approx 2.497 \times 52.796 = 131.86\%$$

- Sample 3:

$$CaCO_3 \approx 2.497 \times 59.132 = 147.66\%$$

The occurrence of values above 100% indicates that this approach does not represent the direct mineral content, but rather reflects the relative degree of carbonate enrichment based on calcium. This may be explained by the fact that calcium is present not only in $CaCO_3$, but also in other Ca-bearing phases, or by the possibility that the XRF data were reported in normalized elemental form. Therefore, this parameter is more appropriately interpreted as an “approximate carbonate equivalent.”

Comparative Interpretation of the Silicate Index. According to the formula

$$SI = \frac{Si+Al}{Ca} \tag{6}$$

the following values were obtained:

- Sample 1:

$$SI = \frac{27.233 + 5.183}{38.731} \approx 0.837$$

- Sample 2:

$$SI = \frac{26.002 + 4.252}{52.796} \approx 0.573$$

- Sample 3:

$$SI = \frac{23.523 + 2.454}{59.132} \approx 0.439$$

These results show that the SI value decreases as mechanical resistance increases. Thus, the sample with low mechanical grade is relatively more silicate-rich, whereas the sample with high mechanical grade is richer in the carbonate component. The decrease in SI may be explained by the predominance of the carbonate phase in the rock matrix, denser bonding between mineral grains, and, consequently, greater structural compactness [3].

Interpretation of the Mineral Strength Index. Based on the formula

$$MI = \frac{CaCO_3}{Si+Fe} \tag{7}$$

the following values were obtained:

- Sample 1:

$$MI \approx \frac{96.73}{27.233 + 16.724} \approx 2.20$$

- Sample 2:

$$MI \approx \frac{131.86}{26.002 + 11.048} \approx 3.56$$

- Sample 3:

$$MI \approx \frac{147.66}{23.523 + 10.087} \approx 4.39$$

The progressive increase in MI demonstrates a direct relationship between the increase in the carbonate component of the chemical composition and the increase in mechanical resistance. This index may therefore be regarded as an integrated parameter reflecting the internal compositional balance of the rock, and it represents an important result of the present study.

FTIR Analysis Results

Table 2. Main FTIR peaks and relative intensities

Sample location	Mechanical grade	ν_3 CO_3^{2-} (cm⁻¹)	Corr.Area (ν_3)	ν_2 (cm⁻¹)	ν_4 (cm⁻¹)	OH zone (cm⁻¹)	Silicate indicator
A	Low	1518–1377	49.021	876	709	3542–3677	589–651
B	Medium	1419	526.209	875	707	3449–3934	1105; 651
C	High	1428	623.114	876	710	3461–3787	652

The FTIR results spectrally confirm the compositional trends identified by XRF. In all samples, the ν_2 and ν_4 vibrations characteristic of the carbonate group were observed at approximately 875–876 cm⁻¹ and 707–710 cm⁻¹, respectively. This reliably confirms the presence of the carbonate phase in the investigated rocks [6].

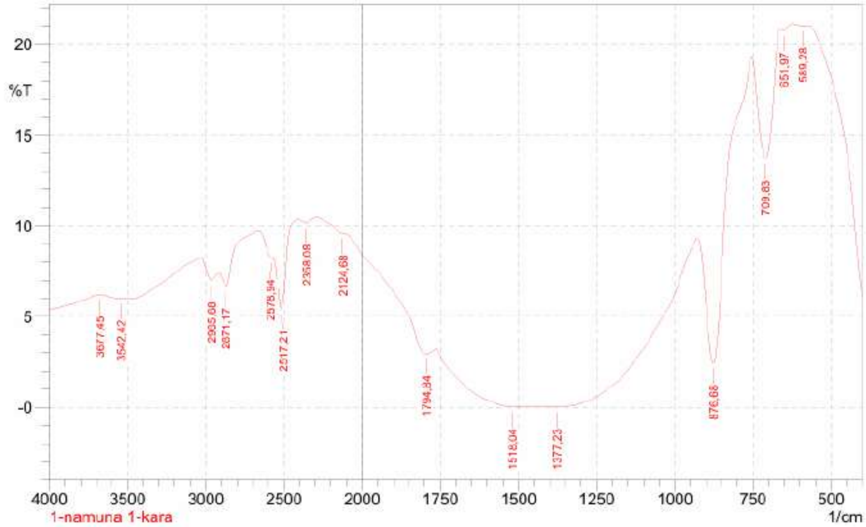

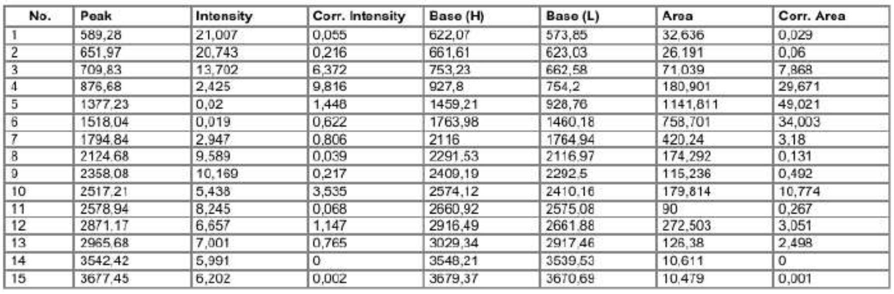

No.	Peak	Intensity	Corr. Intensity	Base (H)	Base (L)	Area	Corr. Area
1	589,28	21,007	0,055	622,07	573,85	32,636	0,029
2	651,97	20,743	0,216	661,61	623,03	26.191	0,06
3	709,83	13,702	6,372	753,23	662,58	71.039	7,868
4	876,68	2,425	9,816	927,8	754,2	180,901	29,671
5	1377,23	0,02	1,448	1459,21	928,76	1141,611	49,021
6	1518,04	0,019	0,622	1763,98	1460,18	758,701	34,003
7	1794.84	2,947	0,806	2116	1764.94	420.24	3,18
8	2124.68	9,589	0,039	2291.53	2116.97	174,292	0,131
9	2358.08	10,169	0,217	2409,19	2292.5	115,236	0,492
10	2517,21	5,438	3,535	2574,12	2410.16	179,814	10,774
11	2578.94	8,245	0,068	2660,92	2575.08	90	0,267
12	2871.17	6,657	1,147	2916,49	2661.88	272,503	3,051
13	2965.68	7,001	0,765	3029,34	2917.46	126,38	2,498
14	3542.42	5,991	0	3548,21	3539,53	10,611	0
15	3677,45	6,202	0,002	3679,37	3670,69	10,479	0,001

A)

The ν_3 region is considered the most important spectral indicator of the carbonate phase. The pronounced variation in the integrated area values within this region among the samples reflects differences in the relative abundance and spectral activity of the carbonate component. In Sample 1, the Corr.Area value was 49.021, whereas in Sample 2 it reached 526.209 and in Sample 3 it increased to 623.114. Therefore, the spectral manifestation of the carbonate phase increased markedly with increasing mechanical grade.

This result is particularly important because the increase in carbonate intensity observed by FTIR is consistent with the increase in Ca content determined by XRF. In other words, the chemical and spectral data corroborate each other. In particular, the high Corr.Area value of Sample 3 indicates that the carbonate phase is better developed or present in greater abundance in the rock with higher mechanical resistance [7].

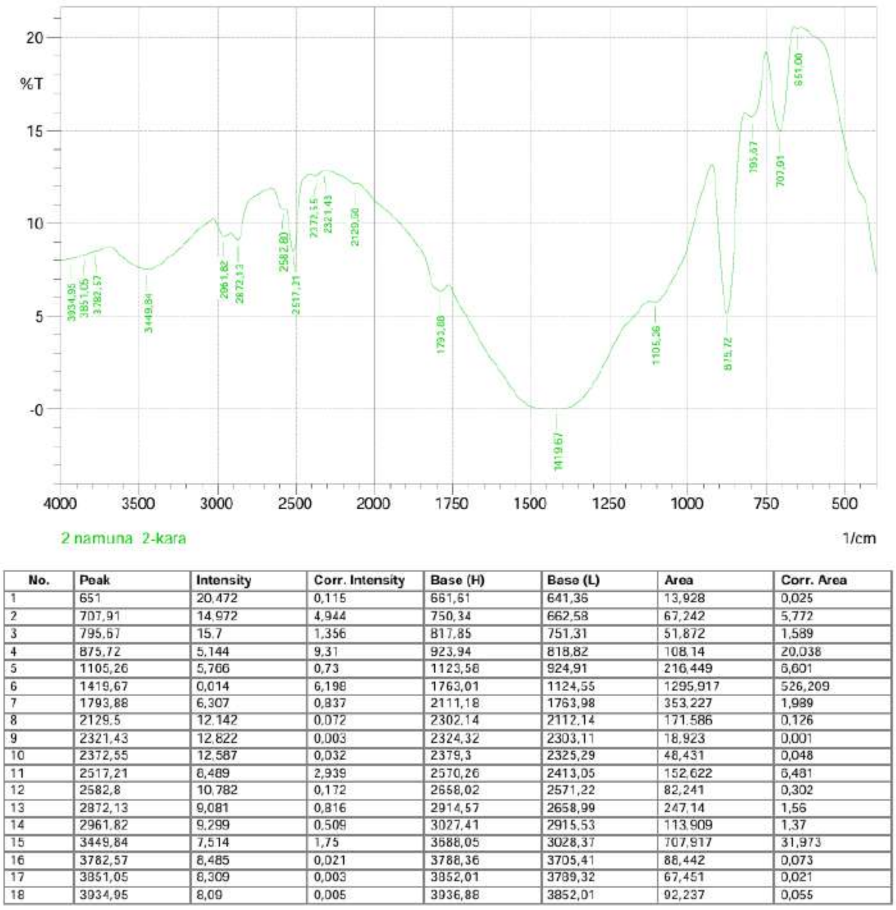

No.	Peak	Intensity	Corr. Intensity	Base (H)	Base (L)	Area	Corr. Area
1	651	20,472	0,115	661,61	641,36	13,928	0,025
2	707,91	14,972	4,944	750,34	662,58	67,242	5,772
3	795,67	15,7	1,356	817,85	751,31	51,872	1,589
4	875,72	5,144	9,31	923,94	818,82	108,14	20,038
5	1105,26	5,766	0,73	1123,58	924,91	216,449	6,601
6	1419,67	0,014	6,198	1763,01	1124,55	1295,917	526,209
7	1793,88	6,307	0,837	2111,18	1763,98	353,227	1,989
8	2129,5	12,142	0,072	2302,14	2112,14	171,586	0,126
9	2321,43	12,822	0,003	2324,32	2303,11	18,923	0,001
10	2372,55	12,587	0,032	2379,3	2325,29	48,431	0,048
11	2517,21	8,489	2,939	2570,26	2413,05	152,622	6,481
12	2582,8	10,782	0,172	2658,02	2571,22	82,241	0,302
13	2872,13	9,081	0,816	2914,57	2658,99	247,14	1,56
14	2961,82	9,299	0,509	3027,41	2915,53	113,909	1,37
15	3449,84	7,514	1,75	3688,05	3028,37	707,917	31,973
16	3782,57	8,485	0,021	3788,36	3705,41	88,442	0,073
17	3851,05	8,309	0,003	3852,01	3789,32	67,451	0,021
18	3934,95	8,09	0,005	3936,88	3852,01	92,237	0,055

B)

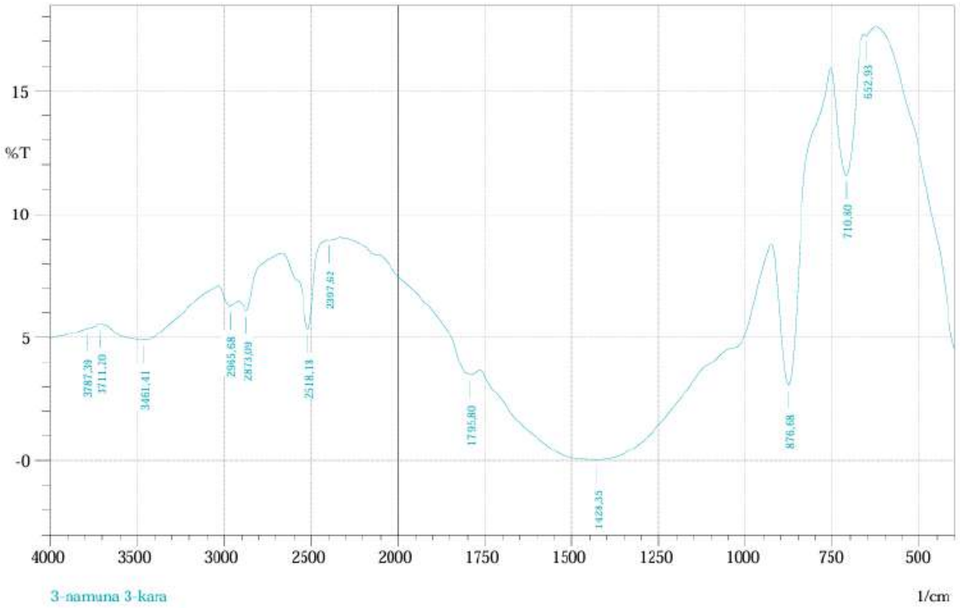

No.	Peak	Intensity	Corr. Intensity	Base (H)	Base (L)	Area	Corr. Area
1	652,93	17,248	0,134	660,65	626,89	25,617	0,039
2	710,8	11,568	5,04	755,16	661,61	80,332	7,46
3	876,68	3,076	7,818	925,87	756,13	181,392	24,427
4	1428,35	0,038	5,702	1763,98	926,84	1664,692	623,114
5	1795,8	3,463	0,509	2331,07	1764,94	654,407	1,806
6	2397,62	8,955	0,022	2410,16	2332,04	81,711	0,076
7	2518,18	5,343	3,385	2665,74	2411,12	287,35	17,088
8	2873,09	6,065	0,768	2916,49	2666,7	281,406	2,257
9	2965,68	6,249	0,505	3030,3	2917,46	133,734	1,908
10	3461,41	4,892	1,217	3708,31	3031,26	846,712	32,493
11	3711,2	5,545	0,001	3716,99	3709,27	9,691	0
12	3787,39	5,372	0,003	3788,36	3717,95	88,988	0,084

C)

Figure 2. FTIR spectra of the chemically analyzed samples

Interpretation of the OH zone. Broad absorption bands were recorded in all samples within the range of 3400–3900 cm^{-1}. This indicates the presence of hydroxyl groups, adsorbed moisture, or certain hydrated mineral phases. Although the OH zone was observed over a relatively wider range in Samples 2 and 3, this feature does not necessarily imply lower strength; rather, it may reflect structural complexity or characteristics associated with surface moisture. Therefore, the OH zone should not be interpreted as an independent criterion, but rather as an auxiliary indicator.

Interpretation of silicate indicators. In Sample 1, silicate indicators were recorded in the range of 589–651 cm^{-1}; in Sample 2, at 1105 and 651 cm^{-1}; and in Sample 3, at 652 cm^{-1}. The peak at 1105 cm^{-1} in Sample 2 is particularly characteristic of Si–O stretching vibrations and indicates a significant contribution of aluminosilicate phases. The relatively more distinct expression of the silicate region in Sample 1 is consistent with its higher SI value. By contrast, the simpler appearance of silicate indicators in Sample 3 suggests the predominance of the carbonate component [8].

Overall, the FTIR results clearly demonstrate the carbonate–silicate nature of the samples and confirm that the spectral role of the carbonate phase becomes stronger with increasing mechanical resistance.

Integrated assessment and scientific discussion. When the XRF and FTIR results are interpreted together, it becomes evident that the degree of mechanical resistance in the rocks of Chortoq District is closely related to their mineral-component composition. In particular, the high-mechanical-grade sample is characterized by a higher Ca content, the lowest SI value, the highest MI value, and a stronger FTIR carbonate signal, all of which indicate a consistent trend [9].

An increase in the carbonate component may enhance the degree of cementation, reduce intergranular voids, and compact the internal structure of the rock. As a result, the rock may exhibit greater resistance to external loading. This behavior is especially typical of dense carbonate-rich or carbonate-cemented rocks. In contrast, relatively higher contents of silicate and iron-bearing components may increase the heterogeneity of the rock and intensify internal microstructural irregularities.

The proposed SI, CI, and MI parameters proved to be convenient criteria for the comprehensive assessment of the rocks:

- SI reflects the silicate-to-carbonate ratio of the rock and indicates the general character of the mineral medium;
- CI expresses the relative spectral activity of the carbonate phase in the FTIR spectrum;
- MI serves as an integrated parameter linking chemical composition with mechanical properties [10–14].

According to the obtained results, the increase in mechanical resistance is characterized by the following general trends: Ca content increases; the relative contents of Si, Al, and Fe decrease; FTIR carbonate intensity increases; SI decreases; and MI increases.

These results indicate that the carbonate component plays a structurally positive role in the investigated samples. However, it should be emphasized that the strength of rocks is not determined solely by chemical composition. Grain size, the presence of microcracks, texture, degree of cementation, porosity, and alteration processes are also important controlling factors. Therefore, XRF and FTIR results provide the greatest scientific value when interpreted together with mechanical test data.

Conclusion. The rock samples collected from the mountainous areas of Chortoq District were comprehensively investigated using XRF and FTIR methods, and their chemical and mineralogical properties were analyzed in relation to their levels of mechanical resistance. The study led to the following scientific conclusions: XRF analysis showed that Ca, Si, Fe, and Al are the major controlling elements in the samples. With increasing mechanical resistance, the Ca content increased, whereas the relative contents of Si, Fe, and Al decreased; the carbonate equivalent calculated on the basis of calcium was significantly higher in the samples with greater mechanical grade. This indicates that the carbonate component has a positive effect on the structural density and strength of the rock; the silicate index (SI) reached its highest value in the low-mechanical-grade sample and its lowest value in the high-mechanical-grade sample [3–5]. This suggests that rocks dominated by silicate components may exhibit relatively lower resistance;

FTIR results confirmed the presence of the carbonate phase in all samples. The identification of the ν_3, ν_2, and ν_4 vibrations, particularly the increase in the integrated area of the ν_3 region in the higher-strength samples, demonstrated the spectral predominance of the carbonate phase; the proposed mineral strength index (MI) increased consistently with increasing mechanical resistance and proved to be a useful integrated parameter expressing the relationship between chemical composition and mechanical properties; the combined interpretation of XRF and FTIR data showed that an increase in the carbonate component is associated with greater rock compactness, stabilization of the internal structure, and improvement in mechanical resistance [6–9]. Thus, the instrumental evaluation of the chemical and mineralogical properties of rocks from Chortoq District provides an important scientific basis for determining their potential as natural construction materials. These results may serve as a foundation for future, more detailed investigations of the physico-mechanical properties, petrographic composition, and service suitability of these rocks.

References

1. Mamahonov.A, Sultanov.D. “Determination of Mechanical Properties of Mountain Rocks in Piedmont Areas of Namangan Region” American Journal of Mechanics and ApplicationsCurrent Issue: Volume 12, Issue 3, September 2025.
2. Mamahonov.A, Sultanov.D. “Determination of physical and mechanical properties of rocks in the village of Hazratishox, Chortoq region”. (Scopus) Physical Research & Engineering Technology Problems – PRETP 2024" P: 030079- 1, 030079-8.
3. Yamasaki, S. I., Yamagishi, H., & Tsuchiya, N. (2023). Major element analysis of geological samples with wavelength-dispersive X-ray fluorescence spectrometry using glass disks and pressed powder pellets. *Journal of the Australian Ceramic Society*.
4. Matsumoto, K., & Fujiwara, K. (1979). Major and trace elements determination in geological and biological samples by energy-dispersive X-ray fluorescence spectrometry. *Analytical Chemistry*.
5. Loubser, M., & Verryn, S. (2008). Combining XRF and XRD analyses and sample preparation to solve mineralogical problems. *South African Journal of Geology*, 111(2–3), 229–238.
6. Bosch Reig, F., Gimeno Adelantado, J. V., & Moya Moreno, M. C. M. (2002). FTIR quantitative analysis of calcium carbonate (calcite) and silica (quartz) mixtures using the constant ratio method. Application to geological samples. *Talanta*, 58(4), 811–821.
7. Stanienda-Pilecki, K. J. (2019). The importance of Fourier-transform infrared spectroscopy in the identification of carbonate minerals. *Spectroscopy Online*.
8. Hahn, A., et al. (2018). Using Fourier transform infrared spectroscopy to determine mineralogical composition of sediment samples. *Sedimentary Geology*.
9. Mroczkowska-Szerszeń, M., et al. (2018). Infrared spectroscopy methods in reservoir rocks analysis: semi-quantitative approach for carbonate rocks. *Nafta-Gaz*, 74(11), 859–866.

10. Wu, D., et al. (2023). Influence of mineral composition on rock mechanics and brittleness of coal measure rocks. *ACS Omega*, 8, 47072–47084.

11. Deng, T., et al. (2024). Mechanical characterization of main minerals in carbonate rocks and their influence on macroscopic behavior. *Processes*, 12(12), 2727.

12. Regnet, J. B., Robion, P., David, C., Fortin, J., Brigaud, B., & Yven, B. (2019). Microstructures and physical properties in carbonate rocks: a review. *Marine and Petroleum Geology*, 103, 73–93.

13. Bakun-Mazor, D., et al. (2024). Predicting mechanical properties of carbonate rocks using spectroscopy across 0.4–12 μm. *Rock Mechanics and Rock Engineering*.

14. Al-Amin, K., et al. (2025). Fourier transform infrared spectroscopic technique for inorganic materials analysis: a review. *Nanoscale Advances*, 7, 4289–4337.

CONTENTS

TECHNICAL SCIENCES: COTTON, TEXTILE AND LIGHT INDUSTRY

TECHNICAL SCIENCES: AGRICULTURE AND FOOD TECHNOLOGIES

CHEMICAL SCIENCES

TECHNICAL SCIENCES: MECHANICS AND MECHANICAL ENGINEERING

ECONOMICAL SCIENCES